

LETTERS

The M2 splice isoform of pyruvate kinase is important for cancer metabolism and tumour growth

Heather R. Christofk¹, Matthew G. Vander Heiden^{1,2}, Marian H. Harris³, Arvind Ramanathan⁴, Robert E. Gerszten^{4,5,6}, Ru Wei⁴, Mark D. Fleming³, Stuart L. Schreiber^{4,7} & Lewis C. Cantley^{1,8}

Many tumour cells have elevated rates of glucose uptake but reduced rates of oxidative phosphorylation. This persistence of high lactate production by tumours in the presence of oxygen, known as aerobic glycolysis, was first noted by Otto Warburg more than 75 yr ago¹. How tumour cells establish this altered metabolic phenotype and whether it is essential for tumorigenesis is as yet unknown. Here we show that a single switch in a splice isoform of the glycolytic enzyme pyruvate kinase is necessary for the shift in cellular metabolism to aerobic glycolysis and that this promotes tumorigenesis. Tumour cells have been shown to express exclusively the embryonic M2 isoform of pyruvate kinase². Here we use short hairpin RNA to knockdown pyruvate kinase M2 expression in human cancer cell lines and replace it with pyruvate kinase M1. Switching pyruvate kinase expression to the M1 (adult) isoform leads to reversal of the Warburg effect, as judged by reduced lactate production and increased oxygen consumption, and this correlates with a reduced ability to form tumours in nude mouse xenografts. These results demonstrate that M2 expression is necessary for aerobic glycolysis and that this metabolic phenotype provides a selective growth advantage for tumour cells *in vivo*.

Otto Warburg noted that tumour cells, unlike their normal counterparts, use aerobic glycolysis with reduced mitochondrial oxidative phosphorylation for glucose metabolism, and proposed that this was an early and essentially irreversible step that ultimately led to tumorigenesis¹. A recent study showed that aerobic glycolysis and the enhanced production of lactate in tumour cells, despite long-held beliefs, is not usually due to mitochondrial defects in oxidative phosphorylation³. These findings are consistent with the idea that tumour cells preferentially use glucose for purposes other than oxidative phosphorylation, and that this metabolic switch may be required to support cell growth. Microarray studies have shown that glycolytic genes comprise one of the most upregulated gene sets in cancer^{4,5}. Among those genes significantly upregulated in tumours is pyruvate kinase, which regulates the rate-limiting final step of glycolysis^{4,5}. Four pyruvate kinase isoforms exist in mammals: the L and R isoforms are expressed in liver and red blood cells; the M1 isoform is expressed in most adult tissues; and the M2 isoform is a splice variant of M1 expressed during embryonic development⁶. Notably, it has been reported that tumour tissues exclusively express the embryonic M2 isoform of pyruvate kinase^{2,7}.

To confirm that tumour tissues switch pyruvate kinase expression from an adult isoform to the embryonic M2 isoform, antibodies that distinguish pyruvate kinase M1 from pyruvate kinase M2 (PKM1 and PKM2, respectively) were generated (Supplementary Fig. 1). Mammary gland tissues from MMTV-NeuNT mice, a breast

cancer tumour model, were analysed before and after tumour development for pyruvate kinase isoform expression⁸. As shown in Fig. 1a, the primary pyruvate kinase isoform before tumour development is PKM1; however, the primary isoform from four independent tumours is PKM2. All cell lines examined, including multiple cancer lines derived from different tissues, also exclusively express the M2 isoform of pyruvate kinase (Fig. 1b). Immunohistochemistry of human colon cancer using the PKM1- and PKM2-specific antibodies shows selective expression of PKM1 in the stromal cells and PKM2 in the cancer cells (Fig. 1c).

Given that PKM2 is selectively expressed in proliferating cells, we assessed its importance for cell proliferation via short hairpin

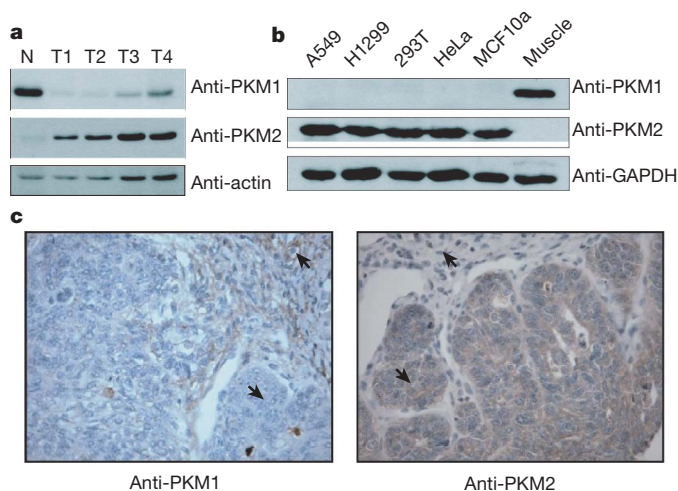


Figure 1 | Tumour tissues and cell lines express the M2 isoform of pyruvate kinase. **a**, Immunoblotting of mammary gland protein lysates from MMTV-NeuNT mice before (N) and after (T) tumour development. T1–T4 represent lysates from tumours that developed in four different mice.

Proteins from total cell extracts were immunoblotted for PKM1, PKM2 and actin. **b**, Immunoblotting of protein lysates from cell lines. A549 and H1299 are lung carcinoma cell lines; 293T is a transformed embryonic kidney cell line; HeLa is a cervical carcinoma cell line; and MCF10a is an immortalized breast epithelial cell line. Mouse muscle lysate was included as a control for M1 antibody staining. Total cell extracts were probed with antibodies towards PKM1, PKM2 and GAPDH. **c**, Immunohistochemistry of human colorectal cancer with antibodies towards PKM1 and PKM2. Stromal cells (arrows pointing upward) stain positive for PKM1; cancer cells (arrows pointing downward) stain positive for PKM2. Images are shown at $\times 400$ magnification.

¹Department of Systems Biology, Harvard Medical School, Boston, Massachusetts 02115, USA. ²Dana Farber Cancer Institute, Boston, Massachusetts 02115, USA. ³Department of Pathology, Children's Hospital, Boston, Massachusetts 02115, USA. ⁴Chemical Biology Program, Broad Institute of Harvard and MIT, Cambridge, Massachusetts 02142, USA. ⁵Cardiology Division and Center for Immunology and Inflammatory Diseases, Massachusetts General Hospital, Boston, Massachusetts 02129, USA. ⁶Donald W. Reynolds Cardiovascular Clinical Research Center on Atherosclerosis, Harvard Medical School, Boston, Massachusetts 02115, USA. ⁷Department of Chemistry and Chemical Biology, Harvard University, Cambridge, Massachusetts 02138, USA. ⁸Division of Signal Transduction, Beth Israel Deaconess Medical Center, Boston, Massachusetts 02115, USA.

(sh)RNA knockdown (Fig. 2a). Stable knockdown of *PKM2* in the human lung cancer cell line H1299 results in decreased rates of glucose metabolism and reduced cell proliferation (Fig. 2b, c). Glucose metabolism was monitored by following the conversion of 5-³H-glucose to ³H₂O, which occurs at the enolase step immediately preceding pyruvate kinase. To address whether it is the M2 isoform that is specifically critical for cell proliferation, we made stable cell lines expressing Flag-tagged mouse PKM1 (mM1) or PKM2 (mM2) and then induced stable knockdown of endogenous *PKM2* using shRNA expression (Fig. 2a). Both mM1 and mM2 were able to rescue the glucose metabolism and proliferation defects of the knockdown cells when grown in the artificially high glucose and oxygen conditions of cell culture (Fig. 2b, c). Similar results were obtained using A549 cells, and no changes in cell size were observed in either cell line (data not shown).

To examine whether *PKM2* expression enhances tumour cell growth under lowered oxygen and glucose conditions, proliferation rates of the M1 and M2 rescue cells (M2 knockdown cells expressing mM1 or mM2) were measured in physiological glucose levels and hypoxic oxygen. Proliferation of neither the M1 nor the M2 cells was affected by growth in normal (5 mM) glucose (data not shown); however, proliferation of the M1 cells was significantly decreased compared to the M2 cells in 0.5% oxygen (Fig. 3a). The per cent decrease in oxygen consumption after addition of subsaturating amounts of oligomycin, a specific inhibitor of mitochondrial ATP synthase, was the same in both the M1 and M2 cells (data not shown). However, oligomycin treatment at the same dose affected the proliferation rate of the M1 cells significantly more than the M2 cells (Fig. 3a). These data suggest that the M1 cells are more dependent on oxidative phosphorylation for cell proliferation.

Consistent with published findings that *PKM1* is a more active enzyme than *PKM2*, we found that the M1 rescue cells had 60%

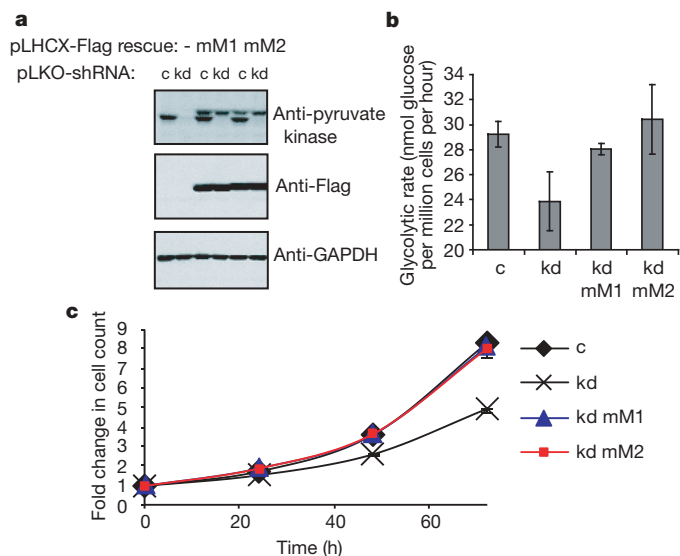


Figure 2 | PKM2 knockdown is rescued by expression of PKM1 *in vitro*. **a**, Immunoblotting of H1299 cells stably expressing shRNA constructs and rescue constructs. Cells were infected with retrovirus containing the empty vector, pLHCX, or pLHCX with Flag-tagged mouse M1 (mM1) or mouse M2 (mM2). After 2 weeks selection in hygromycin, the cells were infected with lentivirus containing the pLKO vector with control shRNA (c) or shRNA that knocks down *PKM2* expression (kd). The cells were then selected in puromycin for 1 week. Total cell extracts were immunoblotted with antibodies for pyruvate kinase (recognizes both M1 and M2), Flag and GAPDH. **b**, **c**, cells with empty rescue vector and control shRNA; kd, cells with empty rescue vector and knockdown shRNA; kd mM1, cells with Flag-mM1 rescue and knockdown shRNA; kd mM2, cells with Flag-mM2 rescue and knockdown shRNA. **b**, Glycolytic rates of the knockdown and rescue cells. **c**, Proliferation curves of the knockdown and rescue cells. Error bars in **b** and **c** denote s.e.m. ($n = 3$).

higher pyruvate kinase activity than the M2 rescue cells (Supplementary Fig. 2a). However, the adenine nucleotide levels in the M1 and M2 cells were comparable in normal culture conditions as well as

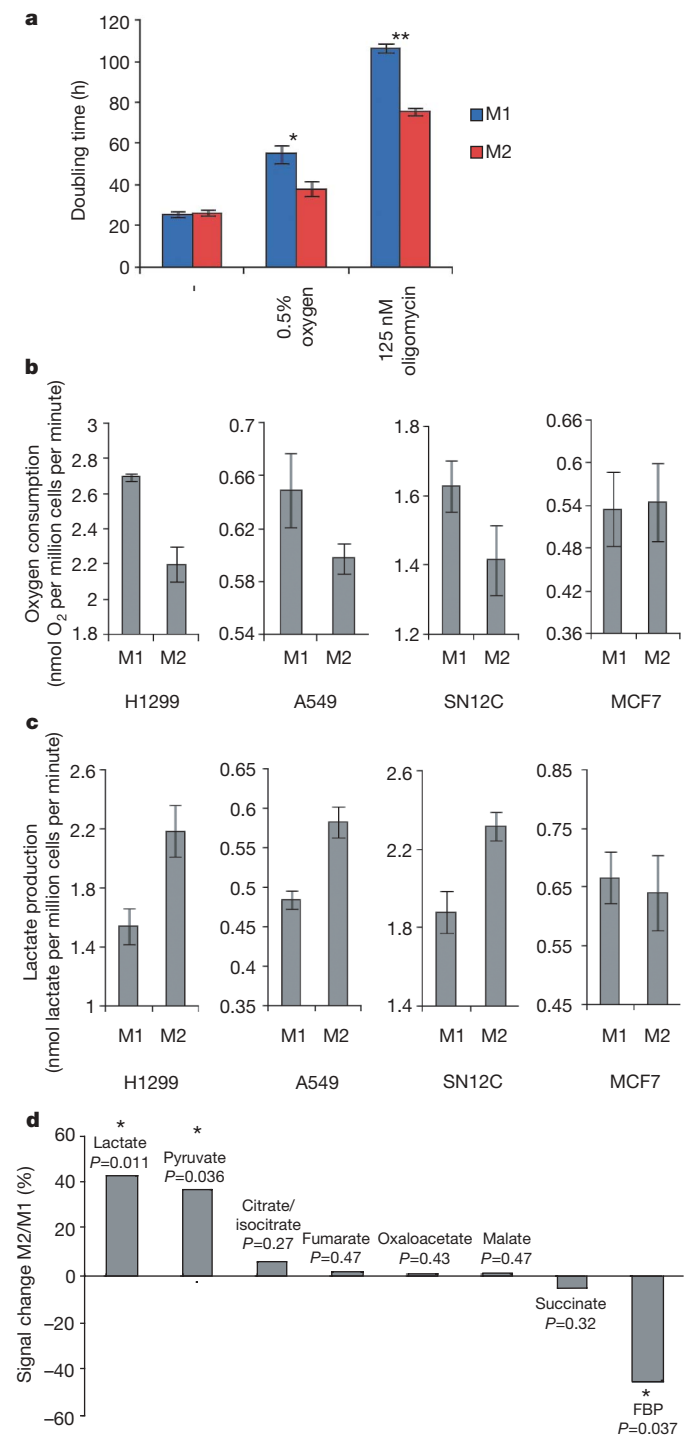


Figure 3 | M1 expression results in increased oxidative phosphorylation. **a**, Doubling times of the M1 and M2 H1299 rescue cells grown in normal oxygen conditions (-), 0.5% oxygen, and in the presence of 125 nM oligomycin. Asterisk, $P = 0.016941$; double asterisk, $P = 0.000048$. **b**, **c**, Data from four different cell lines (H1299, A549, SN12C and MCF7) are indicated. **b**, Oxygen consumption of the M1 and M2 rescue cells. **c**, Lactate production of the M1 and M2 rescue cells as determined by LC-MS. **d**, Metabolite levels in the M1 and M2 H1299 rescue cells as determined by LC-MS. Detected metabolites are represented as the percentage signal change in the M2 versus M1 cells. FBP represents both fructose-1,6-bisphosphate and fructose-2,6-bisphosphate, as the two are undistinguishable by LC-MS. Values were obtained by analysis of six samples. Error bars in **a**, **b** denote s.e.m. ($n = 3$); error bars in **c** denote s.e.m. ($n = 6$).

on treatment with saturating or subsaturating amounts of oligomycin (Supplementary Fig. 2b, c, and data not shown). These data suggest that changes in ATP levels or mitochondrial coupling do not account for the observed changes in proliferation rates in the M1 and M2 cells.

Given the reduced proliferation of the M1 cells in response to both hypoxic conditions and oligomycin treatment, we hypothesized that the M1 rescue cells may preferentially metabolize glucose by oxidative phosphorylation rather than rely on aerobic glycolysis. To test this hypothesis, we compared oxygen consumption, lactate production and metabolite levels in the M1 and M2 rescue H1299 cells. We found that the M1 cells consume more oxygen and produce less lactate than the M2 cells (Fig. 3b, c). These differences in oxygen consumption and lactate production were statistically significant ($P < 0.02$). Similar results were observed when endogenous PKM2 was replaced with mouse PKM1 or mouse PKM2 in two other invasive cancer cell lines, A549 and SN12C (Fig. 3b, c). However, switching pyruvate kinase isoform expression from M2 to M1 in a non-invasive breast cancer cell line known to have low aerobic glucose consumption rates, MCF7⁹, had no significant effect on lactate production and oxygen consumption (Fig. 3b, c).

An increase in lactate levels in the H1299 M2 rescue cells was also found by liquid-chromatography-mass-spectrometry-based (LC-MS) measurement of metabolites (Fig. 3d). Additional metabolite

levels were also different in the M2 cells as compared with the M1 cells. Pyruvate levels were increased and fructose-bisphosphate levels were decreased in the M2 cells (Fig. 3d). Together, these data show that the ratio of lactate production to oxygen consumption is higher in the M2 cells than in the M1 cells and that other glycolytic intermediates are affected by differential expression of these pyruvate kinase isoforms.

To determine whether M2 isoform expression is important for tumour cell growth *in vivo*, we performed xenograft studies using the M1 and M2 rescue cells. Nude mice were injected with 5 million M1 or M2 rescue H1299 cells, and tumour growth was monitored over a 7-week period. As shown in Fig. 4a, mice injected with the M1 cells showed a delay in tumour development as compared with those injected with the M2 cells. Fewer tumours developed from the M1 cells, and those that did were smaller in size (Fig. 4b, c). As judged by total tumour mass, the M2 cells gave rise to significantly larger tumours than the M1 cells (Fig. 4d). Western blot analysis of the developed tumours shows that the Flag-tagged rescue mM1 and mM2 proteins are retained in the tumours; however, endogenous expression of PKM2 returned in both cases (Fig. 4e). No tumours were recovered that solely expressed mM1. To determine whether this was the result of loss of shRNA-mediated knockdown of endogenous PKM2 or whether it represented a selective growth advantage for cells expressing M2, a 50/50 mixture of the M1 and M2 cells was injected into nude mice. Tumours that arose from the mixture of M1 and M2 cells only retained expression of the Flag-mM2 rescue protein, demonstrating that most of the tumour, if not the entire tumour, was derived from the M2-expressing cells (Fig. 4e). These data show that PKM2 expression provides a selective growth advantage for tumour cells *in vivo*.

We show that the switch to the M2 isoform of pyruvate kinase in tumour cells is necessary to cause the metabolic phenotype known as the Warburg effect; however, the mechanism by which this occurs is as yet unknown. Given that PKM2 is expressed during embryonic development and in many non-transformed cell lines, M2 expression alone is unlikely to be a transforming event. Rather, the presence of PKM2 may contribute to a metabolic environment that is amenable to cell proliferation. An attractive hypothesis is that PKM2, which undergoes complex regulation by both fructose-1,6-bisphosphate and protein-tyrosine kinase signalling, provides the flexibility to distribute glucose metabolites into anabolic versus catabolic processes, depending on the demands of rapidly growing cells¹⁰. It remains unclear, however, why more of the pyruvate made in PKM2-expressing cells is converted to lactate whereas more of the pyruvate generated in PKM1 cells is metabolized in the mitochondria. One explanation is that M2 expression results in higher expression of lactate dehydrogenase. Alternatively, M2 expression might lead to reduced mitochondrial density and decreased expression of proteins involved in oxidative phosphorylation. To test these hypotheses, we analysed the expression of the lactate dehydrogenase and F₁F₀-ATPase proteins in the M1 and M2 cells. No differences in the protein levels were detected (data not shown); however, differential activities of lactate dehydrogenase, pyruvate dehydrogenase and/or pyruvate dehydrogenase kinase, or proteins involved in oxidative phosphorylation in the M1 and M2 cells, could account for the observed shift to aerobic glycolysis in the M2-expressing cells.

It is also possible that the M2 isoform of pyruvate kinase has functions independent of its role in glycolysis. GAPDH has been identified to be part of a transcription factor complex¹¹, and a recent study (ref. 12) suggested that the M2 isoform of pyruvate kinase has a role in caspase-independent cell death. In addition, we have recently found that PKM2 has the unique ability among pyruvate kinase isoforms to interact with tyrosine-phosphorylated proteins¹⁰. It is therefore possible that such an alternative function of PKM2 independent of its enzymatic activity promotes aerobic glycolysis and tumour growth.

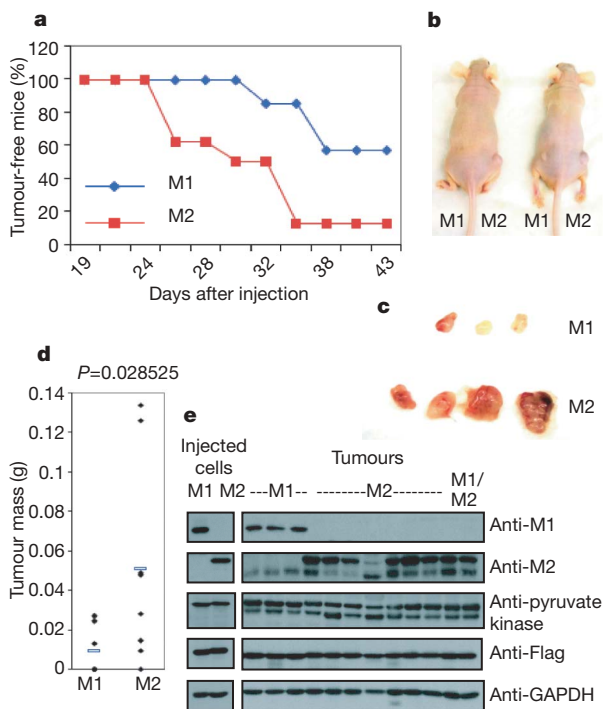


Figure 4 | M1 expression reduces the tumorigenicity of lung cancer cells.

a, Tumour formation over time in nude mice injected with M1 and M2 rescue H1299 cells. After 43 days, 3 out of 7 mice injected with M1 cells and 7 out of 8 mice injected with M2 cells formed tumours. **b**, Mice injected with M1 cells on the left flank and M2 cells on the right flank. The mouse on the left only formed a tumour from the M2 cells. The mouse on the right formed a bigger tumour from the M2 cells than from the M1 cells. **c**, Dissected tumours from the nude mice. The only three tumours derived from M1 cells are shown (top row), and these tumours were smaller than four of the tumours from the M2 cells (bottom row). **d**, Mass of the dissected tumours. Each dot represents the tumour mass from one mouse. The blue line indicates the mean tumour mass originating from M1 cells and M2 cells. **e**, Immunoblotting of tumour lysates originating from M1 cells, M2 cells, or a 50/50 mixture of M1 and M2 cells (M1/M2). The left panel shows lysates from the injected cells. The right panel shows lysates from the dissected tumours. Lysates were immunoblotted with antibodies towards M1, M2, pyruvate kinase (recognizes both M1 and M2), Flag and GAPDH.

Dependence on PKM2-mediated aerobic glycolysis for tumour growth is probably variable in cancer cells given the reliance of some tumours on alternative energy sources such as fatty acid oxidation. This idea is supported by our finding that replacement of PKM2 with mouse PKM1 in the MCF7 cancer cell line had no effect on glucose metabolism as measured by lactate production and oxygen consumption. Glutamine metabolism has also recently been identified as an important source of mitochondrial fuel in cancer cells¹³. It is possible that differences in glutamine metabolism may contribute to the metabolic phenotypes of PKM1 and PKM2 cells.

A well known difference between the M1 and M2 isoforms of pyruvate kinase is that M2 is a low activity enzyme that relies on allosteric activation by the upstream metabolite fructose-1,6-bisphosphate, whereas M1 is a constitutively active enzyme. Additionally, we have recently found that the activity of the M2 isoform (but not the M1 isoform) can be inhibited by tyrosine kinase signalling in tumour cells¹⁰. Decreased M2 activity as a result of growth-factor-stimulated kinase signalling pathways would be predicted to build up phosphoenolpyruvate levels, which would result in inhibition of the isoform of phosphofructokinase-2 expressed in tumour cells, PFKFB3^{14,15}. This would result in reduced fructose-2,6-bisphosphate levels, which would in turn reduce fructose-1,6-bisphosphate levels. This type of regulation is consistent with our results showing a significant reduction in fructose-bisphosphate levels in the M2 cells as compared with the M1 cells. It is therefore possible that differential levels of fructose-bisphosphate, or other upstream metabolites in the glycolytic pathway, mediate the switch to aerobic glycolysis from oxidative phosphorylation in M2-expressing cells by an as yet unexplained mechanism. An alternative explanation is that M1 preferentially shuttles pyruvate to the mitochondria or M2 preferentially shuttles pyruvate to lactate dehydrogenase. For example, tyrosine phosphorylation of lactate dehydrogenase might facilitate its binding to PKM2¹⁰, thereby channelling the product of pyruvate kinase to lactate. Regardless of the mechanism by which PKM2 promotes the Warburg effect, the finding that expression of the M2 isoform is advantageous for tumour cell growth *in vivo* demonstrates that the unique metabolism of tumour cells is critical for tumorigenesis.

METHODS SUMMARY

Cells were lysed in Nonidet P-40 lysis buffer, and western blot analysis was carried out according to standard protocols. Paraffin-embedded colon cancer and control tissues were stained with polyclonal PKM1 and PKM2 antibodies using an automated immunostainer and analysed using immunohistochemistry kits and EDTA-based antigen retrieval (Ventana Medical Systems). For cell line construction, Flag-tagged mouse pyruvate kinase isoforms were cloned into pLHCX and used to make retrovirus to infect H1299, A549, SN12C and MCF7 cells. After 2 weeks of selection in 350 $\mu\text{g ml}^{-1}$ hygromycin (150 $\mu\text{g ml}^{-1}$ hygromycin for MCF7), the stable cells expressing Flag-tagged mouse pyruvate kinase were infected with lentivirus containing knockdown or control shRNA towards human PKM2. These cells were selected for 1 week in 2 $\mu\text{g ml}^{-1}$ puromycin before experimentation. Cellular glucose metabolism rates were measured by following the conversion of 5-³H-glucose to ³H₂O, as described previously¹⁶. Cellular proliferation rates were determined by seeding 5 × 10⁴ cells in triplicate in 6-well plates and taking cell counts every 24 h using a Coulter particle analyser for a 3–5-day period. Pyruvate kinase activity was assessed using a continuous assay coupled to lactate dehydrogenase. Adenine nucleotide levels were measured using an ATP bioluminescence assay kit (Roche) as well as by high-performance liquid chromatography (HPLC), as described previously¹⁷. Lactate production was measured using a fluorescence-based assay kit (BioVision). Oxygen consumption rates were measured using an anaerobic chamber fitted with a polarographic oxygen electrode, as described previously¹⁶. Metabolite extracts were prepared from 2 × 10⁷ cells using cold 80% ethanol, 0.1% formic acid. After centrifugation, the metabolite extracts were dried under nitrogen, reconstituted in water, and analysed by LC-MS as described previously¹⁸. Nude mice were injected subcutaneously with 5 × 10⁶ H1299 cells as described previously¹⁹. Tumour formation was assessed every 2–3 days, and the tumours were dissected and weighed at 7 weeks after injection.

Full Methods and any associated references are available in the online version of the paper at www.nature.com/nature.

Received 18 October 2007; accepted 19 January 2008.

1. Warburg, O. On the origin of cancer cells. *Science* **123**, 309–314 (1956).
2. Mazurek, S., Boschek, C. B., Hugo, F. & Eigenbrodt, E. Pyruvate kinase type M2 and its role in tumor growth and spreading. *Semin. Cancer Biol.* **15**, 300–308 (2005).
3. Fantin, V. R., St-Pierre, J. & Leder, P. Attenuation of LDH-A expression uncovers a link between glycolysis, mitochondrial physiology, and tumor maintenance. *Cancer Cell* **9**, 425–434 (2006).
4. Majumder, P. K. *et al.* mTOR inhibition reverses Akt-dependent prostate intraepithelial neoplasia through regulation of apoptotic and HIF-1-dependent pathways. *Nature Med.* **10**, 594–601 (2004).
5. Altenberg, B. & Greulich, K. O. Genes of glycolysis are ubiquitously overexpressed in 24 cancer classes. *Genomics* **84**, 1014–1020 (2004).
6. Jurica, M. S. *et al.* The allosteric regulation of pyruvate kinase by fructose-1,6-bisphosphate. *Structure* **6**, 195–210 (1998).
7. Dombrauckas, J. D., Santarsiero, B. D. & Mesecar, A. D. Structural basis for tumor pyruvate kinase M2 allosteric regulation and catalysis. *Biochemistry* **44**, 9417–9429 (2005).
8. Muller, W. J., Sinn, E., Pattengale, P. K., Wallace, R. & Leder, P. Single-step induction of mammary adenocarcinoma in transgenic mice bearing the activated *c-neu* oncogene. *Cell* **54**, 105–115 (1988).
9. Gatenby, R. A. & Gillies, R. J. Why do cancers have high aerobic glycolysis? *Nature Rev. Cancer* **4**, 891–899 (2004).
10. Christofk, H. R., Vander Heiden, M. G., Wu, N., Asara, J. M. & Cantley, L. C. Pyruvate kinase M2 is a phosphotyrosine binding protein. *Nature* doi:10.1038/nature06667 (this issue).
11. Zheng, L., Roeder, R. G. & Luo, Y. S phase activation of the histone H2B promoter by OCA-S, a coactivator complex that contains GAPDH as a key component. *Cell* **114**, 255–266 (2003).
12. Stetak, A. *et al.* Nuclear translocation of the tumor marker pyruvate kinase M2 induces programmed cell death. *Cancer Res.* **67**, 1602–1608 (2007).
13. DeBerardinis, R. J. *et al.* Beyond aerobic glycolysis: transformed cells can engage in glutamine metabolism that exceeds the requirement for protein and nucleotide synthesis. *Proc. Natl Acad. Sci. USA* **104**, 19345–19350 (2007).
14. Manes, N. P. & El-Maghrabi, M. R. The kinase activity of human brain 6-phosphofructo-2-kinase/fructose-2,6-bisphosphatase is regulated via inhibition by phosphoenolpyruvate. *Arch. Biochem. Biophys.* **438**, 125–136 (2005).
15. Telang, S. *et al.* Ras transformation requires metabolic control by 6-phosphofructo-2-kinase. *Oncogene* **25**, 7225–7234 (2006).
16. Vander Heiden, M. G. *et al.* Growth factors can influence cell growth and survival through effects on glucose metabolism. *Mol. Cell. Biol.* **21**, 5899–5912 (2001).
17. Budinger, G. R. *et al.* Cellular energy utilization and supply during hypoxia in embryonic cardiac myocytes. *Am. J. Physiol.* **270**, L44–L53 (1996).
18. Sabatine, M. S. *et al.* Metabolomic identification of novel biomarkers of myocardial ischemia. *Circulation* **112**, 3868–3875 (2005).
19. Engelman, J. A. *et al.* Allelic dilution obscures detection of a biologically significant resistance mutation in EGFR-amplified lung cancer. *J. Clin. Invest.* **116**, 2695–2706 (2006).

Supplementary Information is linked to the online version of the paper at www.nature.com/nature.

Acknowledgements We thank M. Bentires-Alj for the MMTV-NeuNT tissue lysates and W. Hahn for the lentiviral shRNA constructs. We thank S. Soltoff for use of the anaerobic chamber and oxygen electrode, and Q. Song for use of the hypoxia chamber. We thank I. Rhee and T. Yuan for help with the nude mouse injections. We thank M. Liu for technical assistance. R.E.G. is supported by funding from the National Institutes of Health, the Donald W. Reynolds Foundation, the Fondation Leducq, and the Broad Institute Scientific Planning and Allocation of Resources Committee. M.G.V.H. is a Damon Runyon Fellow supported by the Damon Runyon Cancer Research Foundation. This research was supported by funding to L.C.C. from the National Institutes of Health. S.L.S. is an Investigator with the Howard Hughes Medical Institute.

Author Contributions M.H.H. and M.D.F. contributed the immunohistochemistry data (Fig. 1c). A.R., R.E.G., R.W. and S.L.S. contributed the metabolite measurement data (Fig. 3d). H.R.C. and M.G.V.H. performed all other experiments. H.R.C., M.G.V.H. and L.C.C. designed the study and wrote the paper.

Author Information Reprints and permissions information is available at www.nature.com/reprints. The authors declare competing financial interests: details accompany the full-text HTML version of the paper at www.nature.com/nature. Correspondence and requests for materials should be addressed to L.C.C. (lcantley@hms.harvard.edu).

METHODS

Cell lysis and immunoblotting. All cell lines were purchased from ATCC and cultured according to ATCC protocols. Cells were lysed in buffer containing 50 mM Tris pH 7.5, 1 mM EDTA, 150 mM NaCl, 1% Nonidet P-40, 1 mM dithiothreitol, 4 $\mu\text{g ml}^{-1}$ aprotinin, 4 $\mu\text{g ml}^{-1}$ leupeptin and 4 $\mu\text{g ml}^{-1}$ pepstatin. After homogenization, mouse tissues were lysed in buffer containing 25 mM Tris pH 7.4, 10 mM EDTA, 10 mM EGTA, 100 mM NaF, 50 mM NaPPi, 1% Nonidet P-40, 1 mM dithiothreitol, 4 $\mu\text{g ml}^{-1}$ aprotinin, 4 $\mu\text{g ml}^{-1}$ leupeptin and 4 $\mu\text{g ml}^{-1}$ pepstatin. Western blot analysis was carried out according to standard methods. The following commercial antibodies were used as probes: pyruvate kinase (Abcam), GAPDH (Abcam), actin (Sigma), Flag (Sigma).

Immunohistochemistry. Archived paraffin-embedded tissue from a patient previously diagnosed with colon cancer and from a normal control (both from Children's Hospital Boston) were stained with polyclonal antibodies to PKM1 and PKM2 using an automated immunostainer and analysed using immunohistochemistry kits and EDTA-based antigen retrieval (Ventana Medical Systems). Results were photographed using an Olympus BX50 microscope and an Olympus QColour3 camera.

Rescue constructs and retroviral production. Flag-tagged mouse PKM1 and PKM2 were cloned into the retroviral vector pLHCX (Clontech) and were co-transfected into 293T cells along with an expression vector with an Amphi cassette. Retrovirus was harvested 36 h after transfection, and 5 $\mu\text{g ml}^{-1}$ polybrene was added. Subconfluent H1299, A549 and SN12C cells were infected with harvested retrovirus and were selected in 350 $\mu\text{g ml}^{-1}$ hygromycin for 2 weeks. MCF7 cells were infected and selected in 150 $\mu\text{g ml}^{-1}$ hygromycin for 2 weeks.

shRNA constructs and lentiviral production. shRNA constructs were provided by W. Hahn (RNAi consortium) in lentiviral cassettes. A shRNA with high pyruvate kinase knockdown efficiency was used (kd) (5'-CCGGGCTGTGGC-TCTAGACACTAACTCGAGTTTAGTGTCTAGAGCCACAGCTTTTGG-3'), and a shRNA with no effect on pyruvate kinase levels was used as a control (cl) (5'-CCGGGAGGCTTCTTATAAGTGTCTTACTCGAGTAAACACTTATAAGA-AGCCTCTTTTGG-3'). As described previously²⁰, lentivirus was made using a three-plasmid packaging system. Briefly, shRNAs in the pLKO.1-puro vector were co-transfected into 293T cells along with expression vectors containing the *gag/pol*, *rev* and *vsf* genes. Lentivirus was harvested 48 h after transfection, and 5 $\mu\text{g ml}^{-1}$ polybrene was added. Subconfluent H1299 and A549 cells were infected with harvested lentivirus, and were selected in 2 $\mu\text{g ml}^{-1}$ puromycin for 1 week.

Measurement of glucose metabolism. Cellular glucose metabolism rates were measured by following the conversion of 5-³H-glucose to ³H₂O as described previously¹⁶. The assay was performed with cells attached to tissue culture plates. Briefly, the cells were washed once in PBS, before incubation in Krebs buffer without glucose for 30 min at 37 °C. The Krebs buffer was then replaced with Krebs buffer containing 10 mM glucose spiked with 10 μCi of 5-³H-glucose. After 1 h, triplicate samples of media were transferred to PCR tubes containing 0.2 N HCl and the amount of ³H₂O generated was determined by diffusion, as described previously¹⁶.

Cell proliferation analysis. 5 × 10⁴ cells were seeded in triplicate in 6-well plates, and accurate cell counts were obtained every 24 h using a Coulter particle analyser for a 3–5-day period. Time zero was taken 16 h after seeding. Cells grown in low oxygen were incubated in a sealed hypoxia chamber set to 0.5% oxygen. Cells

grown in the presence of oligomycin were treated with 125 nM oligomycin at time zero.

Measurement of pyruvate kinase activity. Pyruvate kinase activity was measured by a continuous assay coupled to lactate dehydrogenase (LDH). The change in absorbance at 340 nm owing to oxidation of NADH was measured using a Victor3 1420 Multilabel Counter spectrophotometer (PerkinElmer). Kinetic assays for activity determinations contained cell lysate (1–2 μg), Tris pH 7.5 (50 mM), KCl (100 mM), MgCl₂ (5 mM), ADP (0.6 mM), PEP (0.5 mM), NADH (180 μM), FBP (10 μM) and LDH (8 units).

Adenine nucleotide determination. ATP levels were assessed using an ATP bioluminescence assay kit (Roche). Adenine nucleotides were also measured by HPLC as described previously¹⁷. Briefly, for each sample, 6 million cells were re-suspended in 300 μl of media. Twenty microlitres of 1 M HClO₄ was added and this solution was extracted with 11.75/13.25 (v/v) mixture of tri-*n*-octylamine/fluorotrichloromethane. The aqueous phase was recovered and applied to a Zorbax Rx C8 column and eluted with a linear gradient of 90% buffer A (50 mM KH₂PO₄, 8 mM tetrabutylammonium hydrogen sulphate (TBAS pH 5.8))/10% buffer B (50 mM KH₂PO₄, 8 mM TBAS, pH 5.8, 40% acetonitrile) to 55% buffer A/45% buffer B over 15 min. Adenine nucleotides were detected spectrophotometrically (254 nm). ATP, ADP and AMP peaks within each sample were confirmed by co-injection of each nucleotide with each sample. Standard curves were determined for ATP, ADP and AMP to facilitate quantification of the nucleotides in each sample.

Measurement of oxygen consumption. Cellular oxygen consumption rates were measured using a water-jacketed (37 °C) anaerobic chamber fitted with a polarographic oxygen electrode as described previously¹⁶. The electrode was calibrated with 150 mM NaCl equilibrated to room air at 37 °C (corresponding to 199 nmol O₂ per ml).

Measurement of lactate production. Lactate production was measured using a commercially available fluorescence-based assay kit (BioVision). Fresh media was added to a 12-well plate of subconfluent cells, and aliquots of media from each well were assessed 1 h later for amount of lactate present. Cell number was determined using a Coulter particle analyser.

Measurement of metabolite levels. Metabolite extracts were prepared from 2 × 10⁷ cells using 2 ml ice-cold 80% ethanol containing 0.1% formic acid. Extracts were centrifuged at 10,000 r.p.m. for 20 min at 4 °C, and the supernatant was dried under a nitrogen flow. The dried extract was reconstituted in 400 μl water, and the insoluble fraction was spun down at 10,000 r.p.m. for 20 min at 4 °C. Two-hundred microlitres of the supernatant was loaded into 96-well plates, and the LC-MS analysis of metabolites was performed as described previously¹⁸.

Xenograft studies. Nude mice (nu/nu, male 6–8-week-old, Charles River Laboratories) were injected subcutaneously with 5 × 10⁶ H1299 cells as described previously¹⁹. Tumour formation was assessed every 2–3 days. At 7 weeks after injection, the tumours were dissected and weighed.

Statistical analyses. All *P* values were obtained using an unpaired two-tailed *t*-test.

20. Root, D. E., Hachohen, N., Hahn, W. C., Lander, E. S. & Sabatini, D. M. Genome-scale loss-of-function screening with a lentiviral RNAi library. *Nature Methods* 3, 715–719 (2006).